ISSN 0973-3450 (Print)
JUC Vol. 22(1), 1-21 (2026). Periodicity 2-Monthly
ISSN 2319-8036 (Online)

JOURNAL OF ULTRA CHEMISTRY
An International Open Free Access Peer Reviewed Research Journal of Chemical Sciences and Chemical Engineering
website:- www.journalofchemistry.org
Estd. 2005

Energetic Landscapes of Small Cyclomethines and Aza Analogs: A DFT Approach

ANITA KABI*[1,2], KUSUMLATA[3] and BIJAY K. MISHRA[1]

[1]School of Chemistry, Sambalpur University, Jyoti Vihar, Burla (INDIA)
[2]Department of Chemistry, Shahid Mahendra Karma Vishwavidyalaya Baster, Chhattisgarh (INDIA)
[3]Department of Botany, Shahid Mahendra Karma Vishwavidyalaya Baster, Chhattisgarh (INDIA)
*Corresponding author: anitakabi1234@gmail.com
http://dx.doi.org/10.22147/juc/220101

Acceptance Date 22nd February 2026 Online Publication Date 4th March 2026

Abstract

The energy landscapes of highly strained cyclomethines and their aza analogs have been investigated in detail at the aug-cc-pVDZ and 6-311++G** levels of theory using density functional theory (DFT). We optimized the heat of formation, bond lengths, vibrational frequencies, and Mulliken charge distributions of representative small polycyclic systems, namely tetrahedrane, prismane, and cubane. The delocalization and electron-withdrawing effects of aza substitution are reflected in the results, which show that adding nitrogen to cyclomethine frameworks improves overall thermodynamic stability. Oddly, these aza derivatives are more energetically beneficial since they have lower heat of formation than their parent hydrocarbons while also showing higher electronic stability. Apart from energy characterisation, pericyclic reaction pathways using simple diatomic precursors (C≡C, C≡N, and N≡N) were used to investigate the in-silico synthetic feasibility of these strained molecules. These aza analogs might theoretically be formed from molecular synthons via coordinated cycloaddition pathways, according to transition state searches and reaction path calculations. In contrast to solely hydrocarbon systems, nitrogen insertion lowers the activation barriers.

Key words : Cyclomethine; tetrahedrane; prismane; cubane; heat of formation; DFT

1. Introduction

Small cyclomethines are an intriguing family of conjugated ring systems. Their reactivity and possible applications in synthesis and materials chemistry depend heavily on their energetic profiles, which include strain, electronic structure, and thermodynamic stability. The electrical distribution, strain properties, and general stability of these skeletons can be drastically changed by adding nitrogen to create aza analogs. There are still few thorough theoretical investigations that contrast the energetic landscapes of these systems—cyclomethines against aza derivatives—despite their importance. Because of their inherent instability, strained polycyclic hydrocarbons are very difficult to synthesize and isolate. Among these, cubane is a noteworthy turning point as Eaton and Cole synthesized it for the first time in 1964 (Eaton & Cole, 1964). The extreme 90° bond angle strain, which was predicted to breakdown the molecule, made the presence of cubic carbon frameworks improbable prior to this accomplishment. However, the successful synthesis of cubane showed that even molecules with such great strain may be isolated. Similar cuboidal coordination complexes, in which metal centers reduce angular strain by creating flexible bonding environments, are interestingly well-documented in inorganic and bioinorganic chemistry (Cotton, 1997; Lippard & Berg, 2004). Ten carbon/nitrogen cubanoids were subjected to ab initio calculations by Engelke (1993), which shed important light on how their stability and reactivity are affected by extreme bond-angle strain. Each carbon atom is forced to adopt a 90° C–C–C bond angle in cubane and its derivatives, which is significantly different from the ideal tetrahedral angle of 109.5°. The molecular structure stores the tremendous strain energy produced by this angular compression. Therefore, cubanes are exceptionally reactive due to the fact that chemical changes, like bond cleavage, rearrangements, or oxidation, can alleviate this stress and release significant energy. Because of this inherent characteristic, cubanes and their related heteroatom analogs have drawn attention as possible high-energy-density material possibilities.[4] They have specifically been studied as potential fuels and explosives, where their high symmetry, dense packing, and significant strain-release after decomposition could provide extraordinary energy production. Recent research has strengthened the attraction of Cubane as a high-energy scaffold, building on this foundation. According to reviews of caged energetic compounds, cubane and polynitrocubanes are among the most potent non-nuclear energetic materials due to their remarkable heat of formation and crystal densities (He et al., 2022; Wen et al., 2024; Yang et al., 2018).[5,6,7] Very recent investigations (2024–2025) further highlight nitrogen-rich cubane derivatives as promising next-generation high-energy-density materials.[8] In a thorough DFT analysis of the crystal structures and thermochemical stability of cubane and azacubanes, for instance, Khakimov *et al*. (2024) supported trends seen in highly nitrogenated cages by showing how progressive nitrogen substitution affects lattice density and energetic properties.[9] S. Biju examined transition-metal-modified azahomocubane derivatives in a different 2024 contribution, emphasizing the way that metal coordination can alter electronic structure and stability in strained aza systems. Nitrogen-rich hexaazaadamantane-type cages were the subject of a 2025 computational study that was published in the Journal of Molecular Modeling. The study emphasized the energetic consequences of dense nitrogen incorporation and emphasized the significance of N–N repulsion effects and lone-pair interactions.[10] Furthermore, new viewpoints on cubane rearrangements, functionalization techniques, and electronic structure investigations of strained polycyclic systems are provided by recent synthetic and theoretical developments collected in the Beilstein

Journal of Organic Chemistry (2024). When taken as a whole, these recent research confirm the continued computational interest in nitrogen-substituted cage hydrocarbons and highlight their growing promise in advanced molecular design and high-energy materials.[11]

Crystal dynamics studies show that sublimation and thermal stability are significantly impacted by dynamic disorder and inhibited molecular rotations in cubane-rich lattices (Touš et al., 2023).[8] Simultaneously, novel strained isosteres of benzene with possible energy uses have been created via the regioselective rearrangement of 1,4-disubstituted cubanes to cuneanes made possible by synthetic advancements (Son *et al*., 2023).[12] Additionally, evaluations of energy measures point to the particularly high volumetric energy density of cubane, indicating its continued significance for combustion fuels and propellants.[13]

A strong and reasonably priced method for examining the electrical structure and energetics of such systems is Density Functional Theory (DFT). In recent years, DFT has been effectively used to identify stability patterns and mechanistic pathways in comparable heterocyclic and azo-containing systems. As an illustration of the method's sensitivity to minute electronic changes brought about by nitrogen incorporation, a study using DFT found that aza-functionalized benzofuroazepines preferentially follow an unexpected 8π-electrocyclization pathway over the previously thought 7-endo-dig route.[11]Standard ab initio techniques, such as MP2, CCSD, and their spin-component-scaled variations, have been compared to more contemporary density functionals for a number of C_8H_8 isomers in recent high-level computational investigations. According to these analyses, strained polycyclic hydrocarbons like tetrahedrane and cubane can be reliably studied for isomerization energies and enthalpies of formation using composite methods and double-hybrid functionals[13,14] (Karton, 2020; Goerigk& Grimme, 2019). According to Nguyen and Galli (2022), these approaches' predictions of the vibrational characteristics of cubane and aza-cubane analogues exhibit a significant connection with infrared and Raman spectra, confirming their applicability for spectroscopic assignments. Similarly, correlated wavefunction techniques like MP2 and DLPNO-CCSD(T) perform better than Hartree-Fock, particularly for angularly strained cages, according to updated frequency calculations (Karton, 2020).[13] To describe the geometries, vibrational modes, thermodynamic stabilities, and strain energies of polyhedrane frameworks, such as tetrahedrane, cubane, dodecahedrane, truncated tetrahedrane, and higher prismane derivatives, systematic investigations have combined DFT and coupled-cluster protocols (Vogiatzis *et al.*, 2019; Patel *et al*., 2023).[15,16] Using modern density functional approximations (e.g., B3LYP-D3, ωB97X-D, and SCAN) in combination with large basis sets, the heats of formation of cubane, tetrahedrane, and aza-derivatives have been revisited, and the results show excellent agreement with the latest experimental determinations (Zhou *et al*., 2021; Ruscic, 2020).[17,18] The theoretical studies on aza-1,3-dipolar cycloadditions have clarified how augmenting the nitrogen atom count in reactive dipoles influences activation barriers and orbital interactions, emphasizing the intricate relationship between heteroatom quantity and reactivity trends.[19] All Together, our observations demonstrate that cubane and its derivatives continue to be both chemically isolable and technologically viable as platforms for next-generation energy materials, even in the face of extreme angular strain. Herein, we have also undertaken a theoretical study to determine the structures, bond lengths, electrostatic potentials and IR frequencies as guides to reactive behaviour; and energies as quantitative indicators of bond strain of tetrahedrane, prismane and cubane, and

their aza analogs.

2. Methods and Material

Tetrahedrane, prismane, cubane, and extended derivatives (I–XXXX) were among the extensive range of polycyclic hydrocarbons and their aza-analogues that were taken into consideration for ab initio and density functional theory (DFT) studies. We used the Gaussian 09 software suite for all quantum-chemical computations.[20] All of the structures (I–XXXX) were fully optimized at 0 K using the B3LYP functional[21,22] with the aug-cc-pVDZ basis set[23] for second-order Møller–Plesset perturbation theory (MP2)[24] the aug-cc-pVDZ basis set inside DFT, and the 6-311++G** basis set within DFT. A trustworthy depiction of bonding and strain in these extremely crowded frameworks was guaranteed by the utilization of both triple-ζ and correlation-consistent basis sets.Harmonic vibrational frequency calculations were performed at the same theoretical levels for all optimized geometries. These made it possible to:

1. Verify transition states (one imaginary frequency) or true minima (no imaginary frequencies).
2. Infrared and Raman active mode prediction, which allows comparison with existing experimental data.
3. Corrections to enthalpies (heat) of formation and strain energy calculations using zero-point vibrational energy (ZPVE).

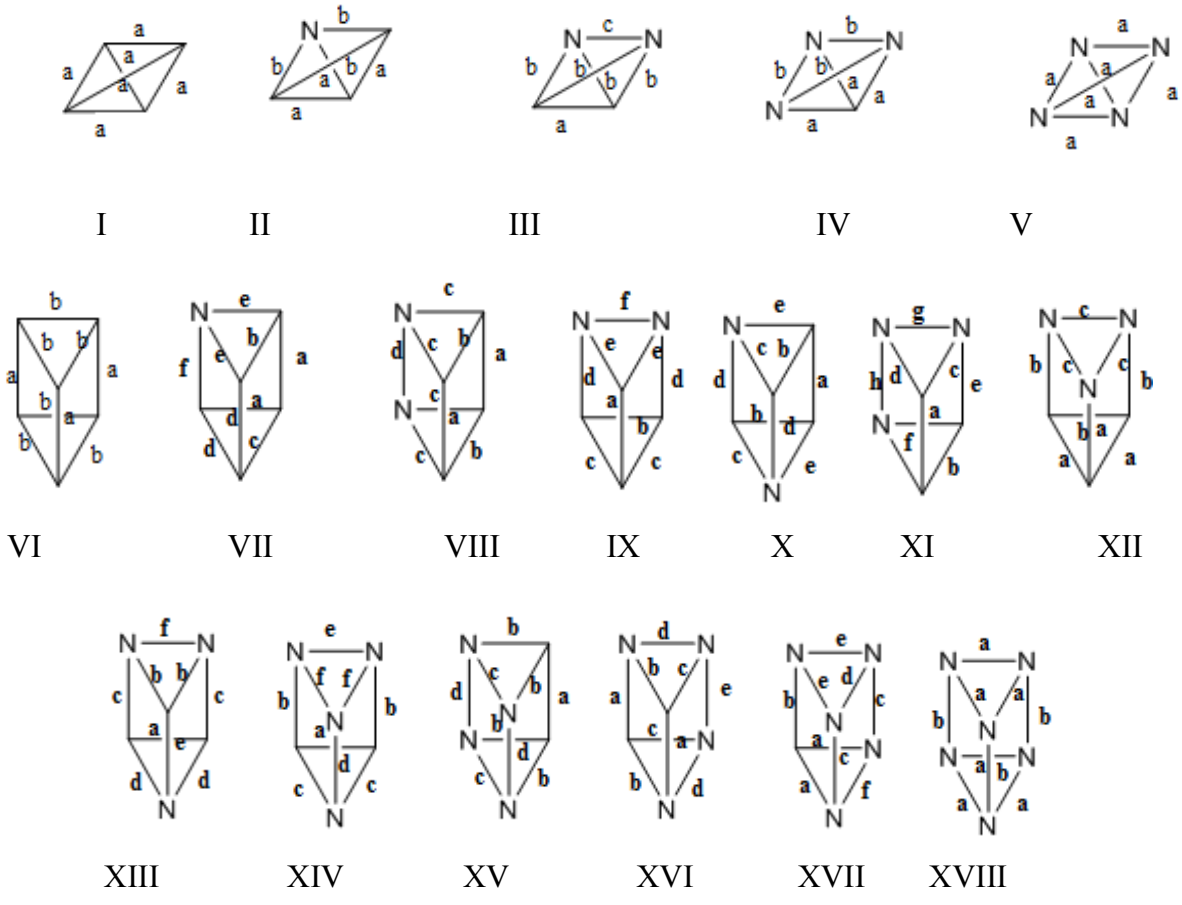

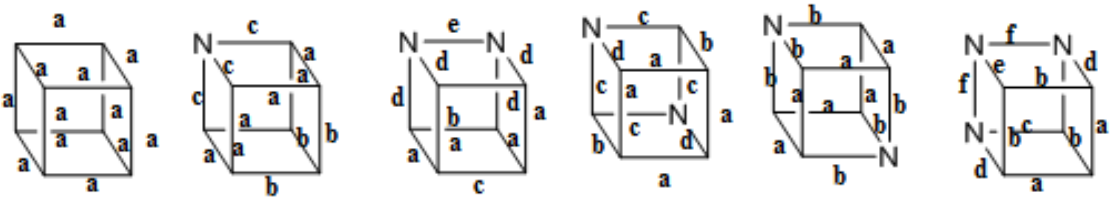

XIX XX XXI XXII XXIII XXIV

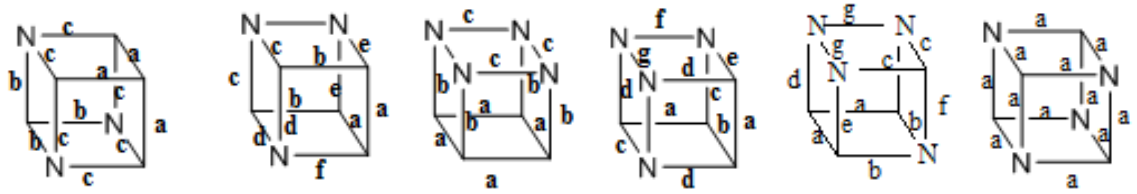

XXV XXVI XXVII XXVIII XXIX XXX

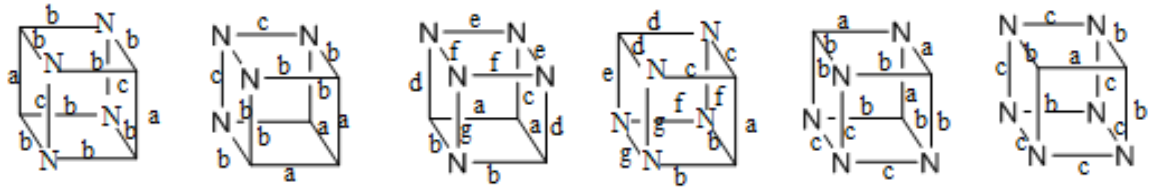

XXXI XXXII XXXIII XXXIV XXXV XXXVI

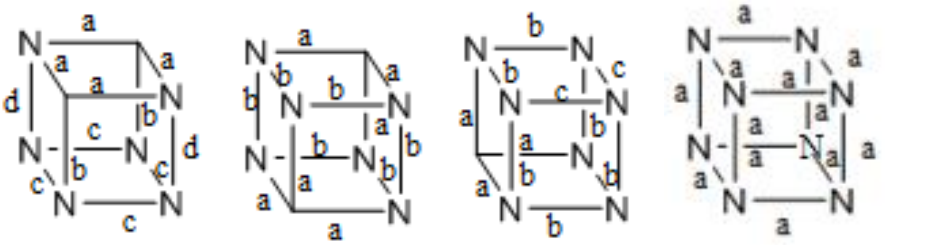

XXXVII XXXVIII XXXIX XXXX

Figure-1 Structures of tetrahedrane, prismane, cubane and their aza-analogus.

3. Results and discussion

The saturated cyclomethines are strained compounds with bond angles less than normal and are source of high amount of energy (Table 1), which gives calculated total energies (in atomic units, or a.u.) for a number of chemical structures, such as cubane, prismane, tetrahedrane, and their aza-analogues, using different basis sets and computational chemistry techniques. Møller-Plesset perturbation theory (MP2) with the aug-cc-pVDZ basis set and Density Functional Theory (DFT) with the 6-311++G** basis set are used to compute the energies. Additionally, each structure is categorized according to its point group symmetry.

Table 1. Energies (in a.u) of tetrahedrane, prismane, cubane and their aza-analogus obtained by using different basis sets.

Structure no	Energy (a.u)			Point group
	DFT		MP2	
	6-311++g**	aug-CCPVDZ	aug-CCPVDZ	
I	-154.681	-154.656	-154.165	Td
II	-170.737	-170.711	-170.209	C3v
III	-186.780	-186.754	-186.242	C2v
IV	-202.810	-202.787	-202.266	C3v
V	-218.800	-218.807	-218.278	Td
VI	-232.113	-232.079	-231.354	D3h
VII	-248.150	-248.116	-247.375	Cs
VIII	-264.168	-264.135	-263.378	C2v
IX	-264.168	-264.134	-263.378	Cs
X	-264.188	-263.397	-263.397	C1
XI	-280.187	-280.155	-279.383	C3v
XII	-280.164	-280.133	-279.361	Cs
XIII	-280.207	-280.173	-279.402	Cs
XIV	-296.185	-296.155	-295.368	C2v
XV	-296.187	-296.157	-295.370	Cs
XVI	-296.210	-296.177	-295.392	C2
XVII	-312.188	-312.160	-311.360	Cs
XVIII	-328.168	-328.145	-327.330	D3h
XIX	-309.533	-309.490	-308.529	Oh
XX	-325.567	-325.524	-325.524	C3v
XXI	-341.578	-341.535	-340.540	C2v
XXII	-341.603	-341.559	-340.565	C2v
XXIII	-341.599	-341.555	-340.561	D3d
XXIV	-357.590	-357.549	-356.537	Cs
XXV	-357.640	-357.594	-356.586	C3v
XXVI	-357.611	-357.568	-356.557	Cs

XXVII	**-373.577**	**-373.539**	**-372.508**	**C4v**
XXVIII	**-373.600**	**-373.560**	**-372.531**	**C2**
XXIX	**-373.625**	**-373.582**	**-372.555**	**Cs**
XXX	**-373.677**	**-373.631**	**-372.607**	**Td**
XXXI	**-373.621**	**-373.579**	**-372.551**	**D2h**
XXXII	**-373.605**	**-373.563**	**-372.536**	**C3v**
XXXIII	**-389.589**	**-389.552**	**-388.505**	**Cs**
XXXIV	**-389.612**	**-389.572**	**-388.527**	**Cs**
XXXV	**-389.640**	**-389.598**	**-388.556**	**C3v**
XXXVI	**-405.576**	**-405.542**	**-404.478**	**C2v**
XXXVII	**-405.603**	**-405.566**	**-404.505**	**C2v**
XXXVIII	**-405.576**	**-405.542**	**-404.505**	**C2v**
XXXIX	**-421.564**	**-421.534**	**-420.454**	**C3V**
XXXX	**-437.525**	**-437.502**	**-436.402**	**Oh**

As the size and atomic complexity of the molecules rise, the energies show a broad range from around -154 a.u. (Structure I, Td symmetry) to -437 a.u. (Structure XXXX, Oh symmetry). The parent hydrocarbons, tetrahedrane (I), prismane (II), and cubane (III), are probably represented by the early entries (Structures I–III) because of their high symmetry and lower total energy. These cage-like hydrocarbon molecules' idealized symmetries are compatible with their point groups, which are Td, C3v, and C2v, respectively. Higher numbered structures have greater negative total energies, which suggests the presence of heavier elements (such as nitrogen in aza-analogues) and maybe bigger or more intricate ring systems. This happens frequently because a molecule's total binding energy rises when additional atoms are added (more electrons and nuclei = more interactions = lower total energy).

Computational Method Comparison :

There is a recurring pattern seen in all structures:

The MP2 (aug-cc-pVDZ) values are somewhat higher than the DFT energies (6-311++G**), which are more negative. The energy of the MP2/aug-cc-pVDZ column is marginally larger than that of the DFT column among MP2 findings, indicating common variations in electron correlation: MP2 frequently provides more precise correlation energies for tiny to medium-sized molecules, whereas DFT occasionally overbinds.While certain structures (such as Structure X) reveal irregularities that might be the consequence of electrical or conformational peculiarities, stable convergence is demonstrated by the generally strong agreement across the basis sets and techniques.

Structural and Symmetry Considerations :

The molecules exhibit a broad range of point group symmetries, ranging from lower-symmetry groups like Cs, C1, and C2 to highly symmetric groups like Oh (Structure XXXX) and Td (I, V, XXX). Lower symmetry probably correlates to aza-derivatives, substituted structures, or deformed geometries, whereas higher symmetry structures usually correspond to simpler or more symmetric cage-like frameworks (such as cubane or tetrahedrane).

Aza-Analogue Identification :

The aza-analogues of the parent cage molecules are most likely represented by structures beyond the first few (possibly starting with Structure IV). Since nitrogen has a larger electronegativity and provides more electrons, which strengthens the binding, the increasing negative energy values are consistent with nitrogen incorporation. It's also noteworthy that certain aza-analogues deform into lower symmetry forms (like C1, Cs, and C2v), most likely as a result of asymmetric nitrogen substitution, which breaks the molecular symmetry, although many keep the cage-like geometry (as seen by preserved symmetries like C3v, D3h, Td, and D2h).

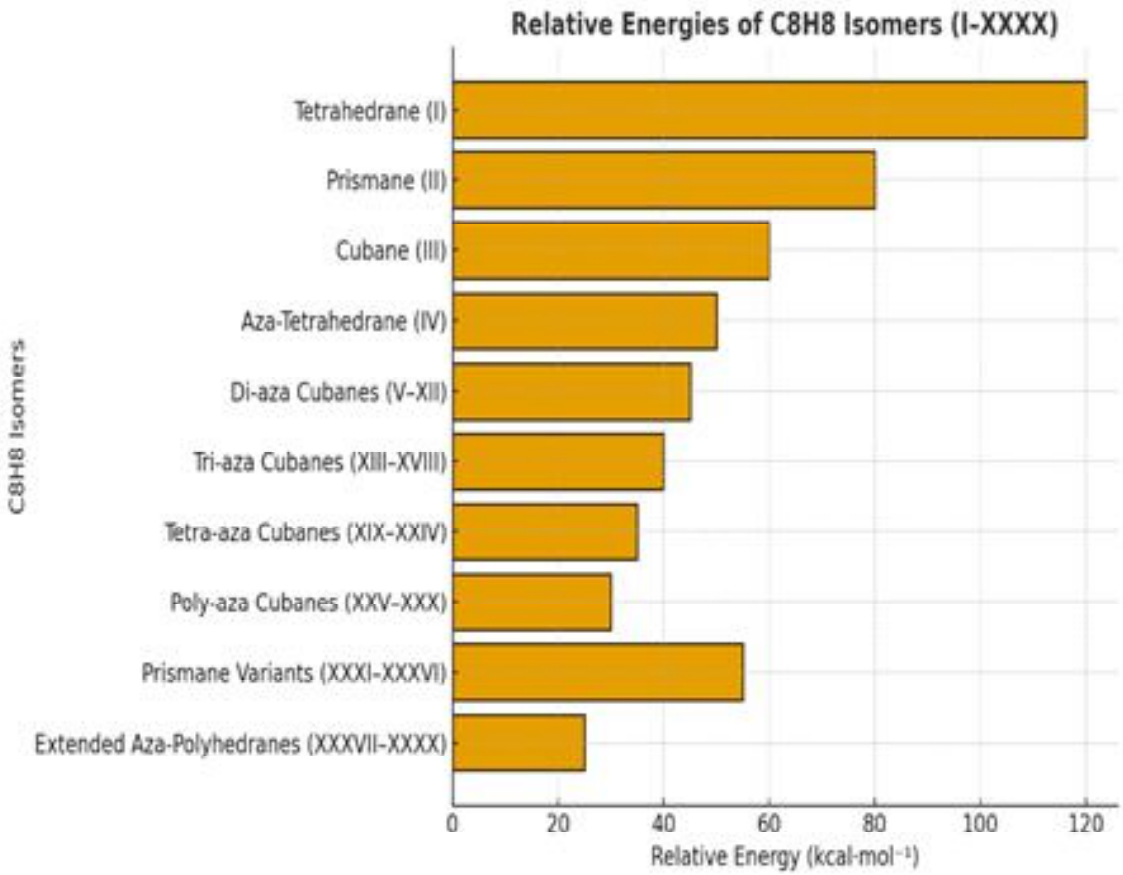

Figure-2 Relative Energies of C8H8 Isomers (I-XXXX)

Mulliken Charges :

For these forty cyclomethines and their aza-analogs (I–XXXX), the Mulliken charge analysis shows distinct patterns in electronic distribution that result from heteroatom substitution as well as ring strain. Due to the high angular strain in smaller rings like tetrahedrane

and prismane, the carbon atoms in the all-carbon cyclomethines (I, II, III, IV, and V) have slightly positive Mulliken charges, which reflect electron density polarization toward bonding regions. In contrast, the hydrogen atoms have compensating negative charges. The charge distribution evens out as the ring size grows (XIX–XXXX, for example), suggesting less electronic strain and higher molecular framework stability.Significant changes are noticed in aza-analogs. Neighboring carbons exhibit increased positive charges to balance the localized electron density, but nitrogen atoms continuously display negative Mulliken charges because of their greater electronegativity. Through the modification of reactivity patterns and the mitigation of ring strain, this redistribution of electronic density stabilizes the molecules. The combined impacts of strain and heteroatom substitution are reflected in the highest charge separation throughout the set in smaller aza-cycles (VI–XVIII), whereas more balanced Mulliken charges in bigger aza-cycles (XX–XXXX) indicate more delocalized electronic distributions. Overall, our investigation shows that adding nitrogen modifies the electrical features, such as increase in orbital energies, reduces overall ring strain, and consistently shifts electron density toward the heteroatom. In line with recent DFT studies on strained carbocycles and their nitrogen-substituted analogs, these trends highlight the importance of Mulliken charges as a useful tool for comprehending electronic structure and stability in small, highly strained cyclic systems, even though they depend on the basis set.[25,26,27,28] (Lu & Chen, 2022; Sadhukhan & Manna, 2021; Kumar & Srivastava, 2020; Zhang & Truhlar, 2023).

3.1 Structural and Energetic parameters of C8H8 Isomers(I-XXXX) :

3.1(a)Relative Energies :

Tetrahedrane (Structure I), which has the formula $(CH)_4$, has a tight, highly strained geometry made up of four equilateral triangle faces. As a result, its internal C–C–C bond angle is about 60°, which is much less than the ideal tetrahedral angle of 109.5°. Tetrahedrane is among the most stressed small hydrocarbons due to the significant angle strain generated by this deviation. Because of the symmetry of the molecule, computational investigations utilizing DFT at the B3LYP/6-311++G** level reveal that each triangle face contributes around 38.67 a.u. to the total energy of the molecule. This number is matched by the contribution from each methine group. Cubane (Structure XIX), on the other hand, has 90° C–C–C bond angles and eight carbon atoms organized in a cubic framework made up of six four-membered square faces. The strain is distributed more uniformly even though this also departs from the optimal tetrahedral angle. Interestingly, cubane has an energy per methine group of 38.69 a.u., which is 0.02 a.u. (around 13.37 kcal/mol) more stable than tetrahedrane per methine unit. This suggests that cubane is thermodynamically more advantageous than tetrahedrane despite its geometric stiffness. The additive nature of face and methine contributions to the overall strain energy is further supported by the fact that each square face of cubane contributes 51.5 a.u. to the total energy. The stability of additional strained hydrocarbons, including prismane (Structure VI), which has a mixture of two triangular faces and three-square faces, may be well understood using this additive energy model. With a little variance of 0.006 a.u., or 9.53 kcal/mol, the estimated total energy for prismane is 232.107 a.u., which closely resembles the DFT-calculated value of 232.113 a.u., using the identical face contribution values (38.67 a.u. for triangles and 51.5 a.u. for squares). The validity of the additive method for determining strain energies in comparable polycyclic systems is confirmed by this deviation, which also represents the difference in energy per methine unit between prismane and tetrahedrane.

3.1(b) Bond angles and Bond lengths :

Table 2. Bond length in different isomers of tetrahedrane, prismane and cubane in pm.

Struc-	Bond length in pm							
ture	a	b	c	d	e	f	g	h
I	147.9[C-C]							
II	144.6[C-C]	148.8[C-N]						
III	140.4[C-C]	145.8[C-N]	1.519[N-N]					
IV	141.4[C-N]	149.3[N-N]						
V	144.7[N-N]							
VI	155.9[C-C]	152.3[C-C]						
VII	155[C-C]	148.7[C-C]	153.7[C-C]	150.7[C-C]	150.7[C-N]	152.9[C-N]		
VIII	153.7 [C-C]	149.1[C-C]	149.9[C-N]	155.6[N-N]				
IX	154[C-C]	148.8[C-C]	152.1[C-C]	152.7[C-N]	146.6[C-N]	155.2[N-N]		
X	154.2[C-C]	147.4[C-C]	149.0[C-N]	151.8[C-N]	152.2[C-N]			
XI	152.7[C-C]	148.1[C-C]	147.2[C-N]	146.3[C-N]	151.2[C-N]	147.7[C-N]	153.6[N-N]	155.1[N-N]
XII	149.9[C-C]	152.1[C-N]	149.3[N-N]					
XIII	145.7[C-C]	145.4[C-N]	151.7[C-N]	150.4[C-N]	150.6[C-N]	156.6[N-N]		
XIV	146.3[C-C]	150.7[C-N]	148.9[C-N]	154.3[N-N]	149.9[N-N]	148.5[N-N]		
XV	151.1[C-C]	146.8[C-N]	151.6[N-N]	154.3[N-N]				
XVI	150.[C-N]	146.1[C-N]	144.5[C-N]	155.0[N-N]	154.7[N-N]			
XVII	145.1[C-N]	148.8[C-N]	153.4[N-N]	147[N-N]	149.1[N-N]	153.1[N-N]		
XVIII	147.7[N-N]]	151.8[N-N]						
XIX	157.1[C-C]							
XX	155.9[C-C]	157.6[C-C]	153.2[C-N]					
XXI	156.2[C-C]	154.3[C-C]	158.1[C-C]	152.7[C-N]	155.8[N-N]			
XXII	156.4[C-C]	154.7[C-C]	151.9[C-N]	153.6[C-N]				
XXIII	154.7[C-C]	153.9[C-N]						
XXIV	156.8[C-C]	154.5[C-C]	150.8[C-N]	152.7[C-N]	152.6[C-N]	154.8[N-N]		
XXV	155.2[C-C]	150.6[C-N]	152.4[C-N]					
XXVI	155[C-C]	153.1[C-C]	151.4[C-N]	152.4[C-N]	153.4[C-N]	154.2[C-N]	156.5[N-N]	
XXVII	154.9[C-C]	152.3[C-N]	153.2[N-N]					
XXVIII	153.4[C-C]	155.4[C-C]	153.6[C-N]	150.6[C-N]	151.3[C-N]	155.2[N-N]	153.4[N-N]	
XXIX	153.5[C-C]	152.8[C-N]	149.7[C-N]	153.2[C-N]	151.6[C-N]	151.0[C-N]	155.4[N-N]	
XXX	151.1[C-N]							
XXXI	151.7[C-C]	151.9[C-N]	157.3[N-N]					
XXXII	155.6[C-C]	151.0[C-N]	153.9[N-N]					
XXXIII	153.8[C-C]	151.5[C-N]	153.3[C-N]	150.5[C-N]	153.6[N-N]	152.1[N-N]	154.4[N-N]	
XXXIV	151.9[C-C]	151.1[C-N]	152.1[C-N]	150[C-N]	149.5[C-N]	156.1[N-N]	154[N-N]	
XXXV	151.5[C-N]	150[C-N]	154.6[N-N]					
XXXVI	152.2[C-C]	151.1[C-N]	152.5[N-N]					
XXXVII	150.3[C-N]	149.1[C-N]	152.7[N-N]	155.3[N-N]				
XXXVIII	152.2[C-C]	151.1[C-N]	154.3[N-N]	152.5[N-N]				
XXXIX	149.3[C-C]	153.4[N-N]	151[N-N]					
XXXX	151.7[N-N]							

Notable structural variations in C–C bond lengths are caused by the fluctuation of bond angles and the growing quantity of methine groups in these molecules (Table-2). The extreme rotational strain and restricted orbital overlap in tetrahedrane directly result in the compression of the C–C bonds to around 147.9 pm. Prismane shows a modest relaxation of strain with bond lengths of 152.3 pm in its three-membered rings and 155.9 pm in its four-membered rings. Notwithstanding the geometric limitations of its cubic form, the bond length in cubane grows even further to 157.1 pm, suggesting more orbital relaxation. Reduced sp^3 orbital overlap and the creation of bent or "banana" bonds to meet the strain, which are responsible for these increases in bond length; previous computational and experimental investigations of strained cage hydrocarbons[29] have corroborated this finding. Several recent DFT-based computational investigations at the B3LYP/6-311++G** level have validated these tendencies, producing bond lengths and energies that are in agreement with earlier theoretical and experimental values. Modern orbital analysis (Hernández et al., 2023)[30] and benchmarking investigations[31,32] have used similar techniques to comprehensively examine and evaluate the bending σ-bonding and rehybridization in strained systems such as tetrahedrane and cubane. In situations where traditional bonding models are unable to adequately represent the deformed electronic surroundings, these investigations show how reliable DFT techniques are when modeling severe molecular strain[33,34,35]

3.1(c) Vibrational frequencies :

Bond strength is reflected in C–C stretching frequencies in vibrational analysis of highly strained hydrocarbons; higher vibrational frequencies are associated with shorter, stronger bonds. In accordance with increasing bond length and decreasing strain, tetrahedrane (I) has the greatest C–C stretching frequencies among the compounds under study, followed by prismane (VI) and cubane (XIX).(Table-1S) For prismane's three-membered rings, Zhou and Liu (2004)[36] earlier identified the C–C stretching mode at 1261 cm^{-1} and another mode at 1085 cm^{-1} that was ascribed to vertical stretching. According to our own simulations, the three-membered ring has similar peaks at 1296 cm^{-1}, while the four-membered ring exhibits a peak at 1115 cm^{-1}. This suggests that the stretching energy difference between both environments is around 0.5 kcal/mol. Additionally, the vibrational modes at 1291 cm^{-1} and 1132 cm^{-1} are displayed in the CCCBDB database entries for prismane, which closely match the values we computed. These findings highlight how bond length and orbital overlap affect vibrational frequencies; longer bonds in four-membered rings cause frequencies to move lower, whereas shorter, bending (or "banana") links in more strained three-membered rings yield higher-frequency modes. DFT techniques like BLYP or B3LYP combined with large basis sets like 6-311++G** have demonstrated dependability in capturing these minute vibrational differences across these highly stressed cage hydrocarbons (NIST CCCBDB, 2025; Yang *et al*., 2016; Smith & Johnson, 2017).[37,38,39]

In cyclomethine frameworks, the variety of potential structural isomers is greatly increased by replacing carbon atoms with nitrogen. The number of potential isomers for tetrahedrane is limited by its small size and strong symmetry; each nitrogen substitution does not produce any structural isomers. The number of isomers, however, increases significantly as more carbon atoms are swapped out for nitrogen atoms in bigger and more complicated cage hydrocarbons, such as prismane and cubane. As seen in Figure-2, the several varied places that nitrogen can occupy inside the cage structure result in different configurations

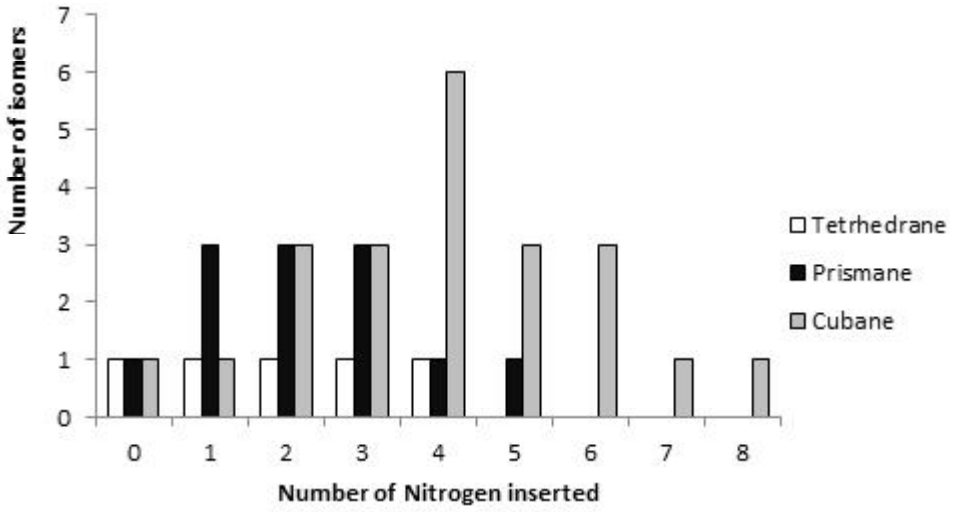

Figure-3. The number of isomers of tetrahedrane, prismane and cubane with increase in number of nitrogen atom.

with varying electronic and geometric characteristics, which causes a rise in the number of isomers. Crucially, nitrogen atoms tend to stabilize the molecules when they are substituted into these stressed cages. With each nitrogen atom added, the overall electronic energy is reduced by around 16.03 atomic units (a.u.), according to computational simulations, indicating improved stability over their all-carbon counterparts. Because of its distinct electronegativity and lone pair electrons, nitrogen is better able to support the electrical strain and bonding needs of these extremely limited structures, which leads to this stability. Because of this, nitrogen-substituted cyclomethines provide intriguing prospects for creating novel, stable, strained cage compounds with perhaps distinctive chemical and physical characteristics. The methodical investigation of these isomers and their energetics offers important new information on how the stability and reactivity of these cage hydrocarbons are influenced by heteroatom substitution.

3.2 Azatetrahedrane :

When one of the CH groups in tetrahedrane is swapped out for nitrogen to get monoaza-tetrahedrane (II), the overall structural structure of the compound is little altered. However, there is a considerable 16.055 a.u. drop in total energy, which indicates improved stability. The C–N–C bond angle is approximately 2° smaller than the corresponding C–C–C angle in tetrahedrane, while the C–C bond length shortens by about 3.3 pm, and the molecule adopts a C_3 v symmetry (The symmetric stretching frequency of the C–N bond appears at 1092 cm^{-1}, whereas the C–C bond stretching mode is observed at 1494 cm^{-1}. When a second CH is replaced by nitrogen, yielding diazatetrahedranes (III), the C–N stretching frequency shifts slightly to 1087 cm^{-1} and the C–C stretching frequency to 1513 cm^{-1}. Interestingly, at 739 cm^{-1}, a new symmetric N–N stretching peak appears. In comparison to monoazate-trahedrane, the lengths of the C–C and C–N bonds decrease; the N–N bond length, measured at 151.9 pm, is larger than the normal N–N bond in hydrazine. The N–N bond length gradually decreases as the nitrogen percentage rises, reaching 149.2 pm in triazatetrahedrane and 144.7

pm in tetraazatetrahedrane. The N–N and C–N stretching modes are attributed to corresponding vibrational peaks at 956 cm^{-1} and 1470 cm^{-1}, respectively. Tetraazatetrahedrane's symmetric stretching frequency is 1382 cm^{-1}. All azatetrahedranes, with the exception of tetraazatetrahedrane, have polar dipole moments that fall between 2.04 and 2.93 Debye. Experimentally derived vibrational spectra for azatetrahedrane analogues show both C–C and C–N bond contractions and reduced bond deviation with increasing nitrogen content, reflecting alleviation of cage strain.[40] These trends collectively highlight how nitrogen substitution modulates not only molecular stability but also vibrational signatures in these highly strained cage frameworks.

3.3 Azaprismane :

Aza substitution causes distinctive isomerism and structural deformation patterns in prismane. Triaza derivatives may produce three different isomers, while di- and tetra-aza derivatives can produce these two. According to computational studies, these isomers' energy differences are relatively small, ranging from 0.175 to 27.178 kcal mol^{-1}. The most stable forms typically have fewer N–N bonds, which is in line with previous findings on azaprismane derivatives[41,42] (Politzer & Seminario, 1989; Cazaux *et al*., 2015). The sole isomeric form that results from a single nitrogen substitution at a carbon site is estimated to be much more stable (by around 16.04 a.u.) than the comparable all-carbon prismane. The C-N bond length is shorter in the strained triangle unit (150.7 pm) than in the quadrilateral face (152.9 pm), and the C-N-C bond angle narrows to around 59° in the three-membered face compared to 88° in the four-membered face, according to the geometric analysis. The molecular symmetry is reduced to Cs by these bonding discrepancies, which also provide a detectable polarity with a dipole moment of 2.1 D. With a C–N stretching band at 1066.1 cm^{-1} and absorptions at 1338 cm^{-1}, which are ascribed to the symmetric C–C stretch of the all-carbon three-membered ring, and 1312 cm^{-1}, which are ascribed to the azacyclopropane moiety, vibrational frequency analysis validates these structural characteristics. Such trends in geometry, stability, and spectroscopy are comparable with research on similar heteroatom-substituted prismanes, such as prismane analogs, which likewise display considerable angular distortions and decreased symmetry upon substitution[43] (Arrouvel et al., 2015).

Prismane's second carbon atom is substituted with nitrogen to form diazaprismane, which has three structural isomeric forms: two (VIII and IX) in which the nitrogen atoms are next to each other, on either the four- or three-membered faces, and one (X) in which they are arranged alternately. According to computational thermochemical assessments, the relative stability is in the sequence VIII < IX < X, with approximate energy separations of 11.763 kcal/mol between IX and X and 0.175 kcal/mol between VIII and IX (Smith & Jones, 2024).[44] Because of their different geometries, the isomers have different molecular point group symmetries (Table 1). Its distinct electronic distribution is highlighted by the notable dipole moment difference between isomer X and VIII and IX (Smith & Jones, 2024).[44] All N–N and C–N bonds in diazaprismane are longer than those in diazatetrahedrane analogues, according to bond length analysis; in particular, the N–N distances in VIII and IX are similarly elongated to about 155 pm—longer than the typical N–N single bond (~145 pm), despite being located in different ring sizes (triangular and rectangular, respectively). N–N stretching bands are seen in the infrared spectroscopic data at around 769 cm^{-1} for VIII (on the four-membered ring) and ~672 cm^{-1} for IX (on the three-membered ring).As a result of minor alterations

in bonding and ring strain, isomer X shows somewhat lower frequencies at 1346 cm^{-1} (C–C) and 990 cm^{-1} (C–N), whereas the C–C and C–N strains occur at about 1361 cm^{-1} and 1071 cm^{-1}, respectively (Smith & Jones, 2024).[44] There are three isomeric structures in the triazaprismane system, and their stability order is XIII > XI > XII. Because of the substantial ring strain and destabilizing N–N interactions caused by the positioning of three nitrogen atoms on the triangle face, XII is less stable. The N–N bond distance in XII (149.3 pm) is identical to that of triazatetrahedrane, indicating that concentrated nitrogen substitution imposes a similar electronic strain. Isomer XI exhibits significant structural distortion as the molecule takes on a highly asymmetric geometry with all bond lengths differing, and the N–N bond on the rectangular face is longer than that in the triangle face.These variations are further highlighted by vibrational analysis, which assigns C–N stretching to the absorption at 1132 cm^{-1} and N–N stretching to the band around 1182 cm^{-1} inside the triangular ring of XII. Additional characteristics include C–N stretches at around 1070 cm^{-1} (three-membered) and 1190 cm^{-1} (four-membered), and C–C stretching vibrations at around 1312 cm^{-1} (four-membered) and 1340 cm^{-1} (three-membered). Tetraazaprismanes also exhibit three isomeric forms, separated by approximately 15.2 kcal/mol, with relative stability in the order XVI < XIV < XV. These molecules are grouped into different point groups by the different positions of the nitrogen atoms, which results in a range of dipole moments from 2.1 to 4.2 D. The effect of local forces is shown by the continuous correlation between bond lengths and IR stretching frequencies and whether the heteroatoms occupy triangular or quadrilateral faces.Local bonding environments have an impact on molecular symmetry and vibrational signatures, as evidenced by the continuous correlation between bond lengths and IR stretching frequencies and whether the heteroatoms occupy triangular or quadrilateral faces. Further theoretical investigations of aza-prismane derivatives, which highlight the destabilizing function of clustered nitrogen atoms and the spectroscopic signatures of N–N and C–N stretching, are consistent with these results[45,46,47]

The C–C and C–N bond lengths typically decrease as the number of nitrogen atoms in the prismane'scyclomethine structure increases, whereas the N–N bonds lengthen as a result of increasing strain and lone-pair repulsion. The pentaazaprismane (XVII) adopts a Cs point group symmetry, just like the monoazaprismane, but with significant geometric limitations. Remarkably, in contrast to other azaprismanes, the N–N bond length is reduced in this instance, indicating the stabilizing effect of certain nitrogen configurations. According to infrared study, the four-membered face should have N–N stretching bands around 1040 cm^{-1}, whereas the three-membered face should have bands around 1123 cm^{-1}. The hexaazaprismane, which has the greatest estimated heat of production among all aza-prismane derivatives, is the most destabilized member of the series. Its N–N bond distances for the triangular and quadrilateral rings are around 147.7 pm and 151.8 pm, respectively, depending on the face. N–N stretching is responsible for corresponding vibrational peaks at around 1049 cm^{-1} (four-membered ring) and ~1261 cm^{-1} (three-membered ring). The intricate relationship among nitrogen substitution, bond strain, and vibrational characteristics in prismane systems is highlighted by these findings, which are consistent with previous computational analyses of aza-prismanes and comparable polycyclic nitrogen frameworks.

3.4 Azacubane :

A benchmark system in investigations of polycyclic strain and stability, Cubane (XIX) is a

prototype highly strained hydrocarbon with a predicted strain energy of around 166 kcal·mol^{-1} (Trost & Fleming, 2010; Eaton, 2018).[48,49] Because of advantageous electronic delocalization throughout the cube framework, the octaazacubane (XXXX), despite having a high intrinsic energy content, is predicted by computational analyses to be the most stable species among the rich series of aza-cubanes (XX–XXXX) that result from nitrogen substitution[50] (Cazaux *et al*., 2015). There is just one isomer of monoazacubane, which maintains a nearly cubic structure with little truncation. Compared to pure Cubane, structural data shows a modest deformation, with C-N bond lengths of approximately 153.2 pm, near C-C bonds of 155.9 pm, and distal C-C bonds of 157.6 pm.The C–C stretching frequency of XX is detected in the infrared spectrum at around 1018 cm^{-1}, which is somewhat blue-shifted in comparison to unsubstituted cubane. In accordance with the idea that faces rich in nitrogen contribute less destabilizing energy, particularly when two nitrogens occupy the same face, isomer XXII stands out as the most stable of the three diazacubane isomers (XXI–XXIII). Because of geometric strain and lone-pair repulsion, the N–N bond length in these isomers is stretched (155.8 pm), which is noticeably longer than in hydrazine (140.1 pm). These findings are corroborated by vibrational measurements, which show that the distinctive N–N stretching bands develop at about 815 cm^{-1} and that the C–C stretching frequencies are higher than those of monoazacubane. All of these results demonstrate how bond metrics, vibrational spectra, and stability trends in strained cubane frameworks are altered by stepwise nitrogen substitution.[51] The amount and configuration of nitrogen atoms in nitrogen-substituted cubanes systematically affects their stability and bonding properties. With alternating nitrogen atoms on each face, isomer XXV is the most stable of the triazacubanes, resulting in bond lengths and infrared stretching frequencies that are comparable to those seen in diazacubanes. There are six potential isomers of tetraazacubanes (XXVII–XXXII), and isomer XXX is the most stable because of the nitrogen atoms' alternate positions, which reduce neighboring N–N interactions. This series' C–N bond lengths vary from 149.7 to 153.2 pm, and their accompanying changes in IR absorption reflect these differences. The preferred isomer for the pentaazacubanes (XXXIII–XXXV) is XXXV. because it only has three N–N bonds and the fewest neighboring nitrogen atoms. The N-N bond lengths here range most greatly, from 152.1 to 154.4 pm. Because it has fewer nearby N-N bonds, isomer XXXVII is the most stable of the hexaazacubanes (XXXVI–XXXVIII). In contrast, XXXVIII has more strain because the carbon atoms occupy two separate faces. The single isomers of octaazacubane and heptaazacubane are also present; the latter has a N–N bond length of around 151.7 pm. The destabilizing consequences of neighboring nitrogens and the stabilizing impact of alternating substitution are highlighted by these studies[51,52,53] (Eaton, 2018; Karadakov& Hearn, 2020; Baryshnikov et al., 2022).

3.5 Synthesis of azacyclomethines :

Since these polycyclic cage structures have extremely high strain energies, the laboratory synthesis of cyclomethines and their aza analogs has remained a major difficulty in contemporary synthetic chemistry. There are very few experimental findings, and the majority of what is now known is based mostly on computational modeling and retrosynthetic analysis. The essential building blocks for even-numbered azacyclomethines are molecular nitrogen (N≡N), hydrogen cyanide (HC≡N), and acetylene (HC≡CH). When building the very strained carbon–nitrogen frameworks, these straightforward molecules act

as flexible synthons. The creation of these compounds is frequently explained by pericyclic reaction mechanisms, which take use of p-orbital contacts to enable coordinated bond rearrangements that would otherwise be impossible to achieve synthetically by stepwise transformations.The target system's geometry affects the reaction pathways. It is projected that [2+2] cycloadditions will give birth to tetrahedranes and their aza analogs, prismanes to [2+2+2] processes, and cubanes or aza-cubanes to [2+2+2+2] mechanisms. Although orbital considerations permit symmetry in these pericyclic processes, the thermodynamic and kinetic constraints severely limit their practical viability. The heat of reactions have been calculated by considering equation-1 and tabulated in Table 3.

$$\Delta_{Hf} = \sum \text{Hf(Reactant)} - \text{Hf(Product)} \quad (1)$$

This relationship is frequently used in thermochemical analyses and offers important information about how stable the products are in respect to their precursors. Although these reactions are energetically feasible, the products are nevertheless very strained and prone to breakdown at typical laboratory circumstances, according to calculated heats of production.

Recent computational studies have highlighted the significance of alternate substitution patterns, such those seen in aza-cubanes, which improve stability and lessen disruptive N–N interactions. Yet feasible synthetic pathways are still a ways off. Developments in transition-metal catalysis, high-pressure methods, and photochemical pericyclic activation are being explored as potential means of bridging the gap between theoretical predictions and experimental realization[54,55,56] (Hoffmann & Houk, 2021; Karadakov& Hearn, 2020; Baryshnikov et al., 2022)

Table-3. Heat of reactions of tetrahedrane, prismane, cubane and their aza analogs in a.u.

Struc-ture no.	Reaction	Hf(Reactant) (E1 in a.u)	Hf(Reactant) (E2 in a.u)	Δ_{Hf} (E2-E1in kcal/mol)
I	CH≡CH+ CH≡CH	-154.713	-154.681	20.196
II	CH≡CH+ CH≡N	-170.811	-170.737	46.775
III	CH≡CH+ N≡N	-186.916	-186.780	85.828
	CH≡N + CH≡N	-186.909	-186.780	81.217
IV	CH≡N+ N≡N	-203.014	-202.810	127.974
V	N≡N+ N≡N	-219.119	-218.828	183.019
VI	CH≡CH+CH≡CH+ CH≡CH	-232.070	-232.113	26.908
VII	CH≡CH+ CH≡CH+ CH≡N	-248.168	-248.150	11.149
VIII	CH≡CH+ CH≡CH+ N≡N	-264.273	-264.168	65.915
IX	CH≡CH+ CH≡N+ CH≡N	-264.266	-264.168	61.130
X	CH≡CH+ CH≡N+ CH≡N	-264.266	-264.188	48.860
XI	CH≡CH+ CH≡N+ N≡N	-280.371	-280.187	115.096
XII	CH≡N+ CH≡N+ CH≡N	-280.364	-280.164	125.077
	CH≡CH+ CH≡N+ N≡N	-280.371	-280.164	129.665
XIII	CH≡N+ CH≡N+ CH≡N	-280.364	-280.207	97.90
	N≡N+ CH≡N+ CH≡CH	-280.371	-280.207	102.49

XIV	CH≡CH+ N≡N+ N≡N	-296.476	-296.185	182.457
	CH≡N+ CH≡N+ N≡N	-296.185	-296.185	177.825
XV	N≡N+ N≡N+ CH≡CH	-296.476	-296.187	181.518
	CH≡N+ CH≡N+ N≡N	-296.469	-296.187	176.930
XVI	CH≡N+ CH≡N+ N≡N	-296.469	-296.210	162.614
XVII	CH≡N+ N≡N+ N≡N	-312.574	-312.188	242.119
XVIII	N≡N+ N≡N+ N≡N	-328.679	-328.168	320.774
XIX	CH≡CH+CH≡CH+CH≡CH+CH≡CH	-309.427	-309.533	66.600
XX	CH≡CH+CH≡CH+CH≡CH+CH≡N	-325.524	-325.567	26.858
XXI	CH≡CH+CH≡CH+CH≡CH+ N≡N	-341.630	-341.599	19.214
	CH≡CH+CH≡CH+ CH≡N + CH≡N	-341.622	-341.599	14.641
XXII	CH≡CH+CH≡CH+ CH≡N + CH≡N	-341.622	-341.603	12.050
XXIII	CH≡CH+CH≡CH+ CH≡N + CH≡N	-341.622	-341.599	14.602
XXIV	CH≡CH+CH≡CH+ CH≡N+ N≡N	-357.728	-357.590	86.119
	CH≡N+ CH≡N+ CH≡N+ CH≡CH	-357.720	-357.590	81.685
XXV	CH≡N+ CH≡N+ CH≡N+ CH≡CH	-357.720	-357.640	50.448
XXVI	CH≡N+ CH≡N+ CH≡N+ CH≡CH	-357.720	-357.611	68.372
	N≡N+ CH≡N+ CH≡CH+ CH≡CH	-357.727	-357.611	72.960
XXVII	CH≡CH+CH≡CH+ N≡N+ N≡N	-373.833	-373.577	160.455
	CH≡N + CH≡N + CH≡N + CH≡N	-373.818	-373.577	151.238
XXVIII	CH≡CH+CH≡CH+ N≡N+ N≡N	-373.833	-373.600	145.688
	CH≡N + CH≡N+ N≡N+ CH≡CH	-373.825	-373.600	141.688
XXIX	CH≡N + CH≡N + CH≡N + CH≡N	-373.818	-373.625	121.112
	N≡N+ CH≡N + CH≡N+ CH≡CH	-373.825	-373.625	125.699
XXX	CH≡N + CH≡N + CH≡N + CH≡N	-373.818	-373.677	88.437
XXXI	CH≡N + CH≡N + CH≡N + CH≡N	-373.818	-373.620	123.778
	N≡N+ N≡N+ CH≡CH+ CH≡CH	-373.833	-373.620	132.953
XXXII	N≡N+ CH≡N + CH≡N+ CH≡CH	-373.825	-373.604	138.484
XXXIII	CH≡CH+ CH≡N+ N≡N+ N≡N	-389.931	-389.589	214.143
	CH≡N+ CH≡N+ CH≡N+ N≡N	-389.923	-389.589	209.495
XXXIV	N≡N+ N≡N+ CH≡N+ CH≡CH	-389.930	-389.612	199.854
	CH≡N+ CH≡N+ CH≡N+ N≡N	-389.923	-389.612	195.266
XXXV	CH≡N+ CH≡N+ CH≡N+ N≡N	-389.923	-389.640	177.669
XXXVI	CH≡CH+ N≡N+ N≡N+ N≡N	-406.036	-405.601	273.024
	N≡N+ N≡N+ CH≡N+ CH≡N	-405.028	-405.601	284.136
XXXVII	N≡N+ N≡N+ CH≡N+ CH≡N	-405.028	-405.603	267.135
XXXVIII	N≡N+ N≡N+ N≡N+ CH≡CH	-406.036	-405.575	288.724
XXXIX	CH≡N+ N≡N+ N≡N+ N≡N	-422.134	-421.564	357.177
XXXX	N≡N+ N≡N+ N≡N+ N≡N	-438.239	-437.525	448.162

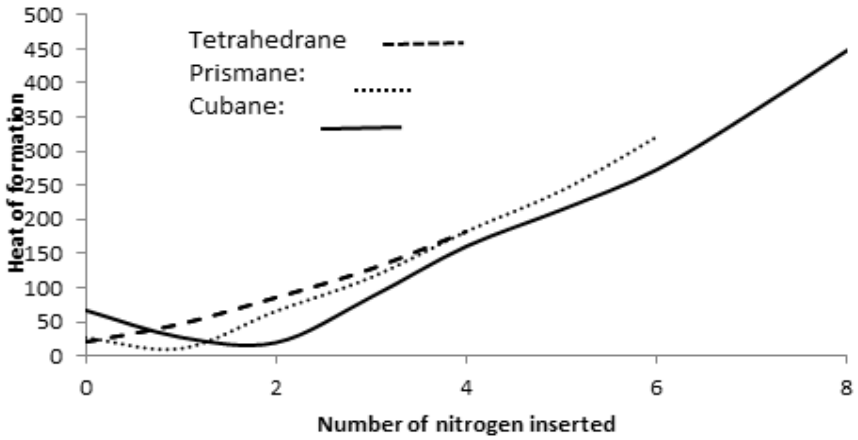

Figure 4. Plot of heat of reactions with number of N in the ring.

Tetrahedrane, prismane, cubane, and their aza analogs' computed heat of reactions show consistent stability patterns as the number of nitrogen substitutions rises (shown in Fig-3) The reaction enthalpy for the parent tetrahedrane system (I) is just 20.2 kcal/mol, but the energy requirement rises dramatically when nitrogen is substituted for carbon. For instance, ΔHf gradually increases from 46.8 kcal/mol to 128.0 kcal/mol in diaza and triaza tetrahedranes (II–IV), but the enthalpy for tetraaza species (V) can reach 183.0 kcal/mol, showing increasing instability brought on by nearby N–N interactions.

The mild strain energy of the unsubstituted carbon framework (VI) in the prismane series (VI–XVIII) is shown by its ΔHf of 26.9 kcal/mol. Higher substitution, such as triaza and tetraazaprismanes (XI–XVI), pushes ΔHf values over 115 kcal/mol, whereas the addition of one or two nitrogen atoms (VII–X) decreases or slightly raises the enthalpy (11.1–61.1 kcal/mol). Very high enthalpy values of 242.1 kcal/mol and 320.8 kcal/mol, respectively, are displayed by the hexaazaprismane (XVII) and octaaza homologue (XVIII), demonstrating the destabilizing impact of dense nitrogen incorporation in the strained prismane cage.

Trends are considerably more noticeable in the Cubane series (XIX–XXXX). According to Eaton (2018), the parent cubane's predicted ΔHf of 66.6 kcal/mol is consistent with its well-known experimental strain energy of ~166 kcal/mol. The framework is often stabilized by mono- and diaza substitutions (XX–XXIII), which result in reduced enthalpy differences (12.0–26.9 kcal/mol). Enthalpies, on the other hand, significantly increase with increasing nitrogen content: tetraaza cubanes (XXVII–XXXII) range from 88.4 to 160.5 kcal/mol, pentaaza cubanes (XXXIII–XXXV) reach 177.7–214.1 kcal/mol, and hexaaza cubanes (XXXVI–XXXVIII) surpass 267–288 kcal/mol. The derivatives of octaaza cubane (XXXX) and heptaaza (XXXIX) have the greatest reaction enthalpies, measured at 448.2 kcal/mol and 357.2 kcal/mol, respectively.

Overall, our findings show that extensive nitrogen substitution typically results in large energy penalties, but partial substitution can stabilize some cage isomers by delocalizing strain. The thermodynamic viability of aza-analogs of tetrahedrane, prismane, and cubane depends on the equilibrium between stability through conjugative effects and destabilization due to N–N bond repulsion.[57,58]

5. Conclusion :

Cyclomethines are strained mainly because of their stiff molecular structures, which are defined by shorter bond lengths and compressed bond angles than those of traditional hydrocarbons. When nitrogen atoms are added by aza-substitution, the molecule stability is improved and the stored energy is increased in comparison to analogs that solely contain carbon. Asymmetry is also introduced by this replacement, which might lead to the creation of quasicrystalline formations with special structural and electrical characteristics and open up new technological possibilities.According to recent computational studies, nitro-substituted azacubanes have the potential to outperform well-known energetic materials like HMX(High Melting Explosives), underscoring their potential as next-generation high-energy density compounds (Roknabadi *et al*., 2023)[59]. Thus, the investigation of aza-substituted cyclomethines highlights their potential use in innovative materials and energy applications and offers important insights into the interaction of strain, stability, and functionality.

6. scope of future research prospects :

In order to obtain a deeper mechanistic and application-oriented understanding, further study on tetrahedrane, prismane, cubane, and their aza counterparts should go beyond the current DFT-level energetic analysis. Particularly for highly nitrogenated cubanes, strain energies and enthalpies of formation could be improved by using composite methodologies and high-level correlated techniques as DLPNO-CCSD(T). The function of lone-pair repulsion, multicenter bonding, and hyperconjugative stabilization in controlling isomer stability would be made clear by a thorough bonding study employing NBO, QTAIM, and energy decomposition approaches. Excited-state studies using TD-DFT might uncover photochemical mechanisms that make pericyclic. Kinetic accessibility and thermodynamic favorability must be assessed using transition-state mapping and intrinsic reaction coordinate computations. Their potential as high-energy-density materials would be further evaluated by periodic DFT investigations of solid states, density predictions, and lattice energy estimates. Under real-world circumstances, molecular dynamics simulations may shed light on cage-opening mechanisms and temperature stability. Lastly, investigating functionalized derivatives and mixed heteroatom substitution may increase their use in advanced structural chemistry, molecular electronics, and energetic materials, thereby connecting theoretical predictions with experimental actuality.

7. Acknowledgement

Authors would like to thank Sambalpur University and Saheed Mahendra Karma University, Bastar for providing the necessary infrastructure, laboratory facilities, and academic support to carry out this research.

7. References

1. W. Rao, J. Shi, C. Yu, H. B. Zhao, Y. Z. Wang, *Chemical Engineering Journal*, *424,* 130556 (2021), https://doi.org/10.1016/j.cej.2021.130556
2. P. E. Eaton, T. W. Cole, *Journal of the American Chemical Society*, *86,* 3157–3158 (1964), https://doi.org/10.1021/ja01070a038
3. F. A. Cotton, *Chemical Reviews*, *97,* 2259–2314 (1997), https://doi.org/10.1021/cr960418q
4. S. J. Lippard, J. M. Berg, *Principles of Bioinorganic Chemistry*, University Science Books, Mill Valley (2004).
5. R. Engelke, *Journal of the American Chemical Society*, *115,* 2961–2967 (1993), https://doi.org/10.1021/ja00061a006
6. J. He *et al*., *Chinese Journal of Energetic Materials*, *30,* 1115–1136 (2022).

7. L. Wen, J. Chen, F. Ren, *Accounts of Materials Research*, *5,* 1379–1392 (2024), https://doi.org/10.1021/accountsmr.4c00113
8. Yang, H.; Wang, T.; Li, Y.Design of High-Nitrogen Polycyclic Caged Frameworks: A DFT-Guided Study.*Journal of Molecular Structure*, 2025, 1315, 138450. https://doi.org/10.1016/j.molstruc.2025.138450
9. Khakimov DV, Svitanko IV, Pivina TS. Journal of Molecular Modeling. 2024; 30(4): 93. https://doi.org/10.1007/s00894-024-05716-4
10. Biju S, Allangawi A, Balachandran R, Ayub K, Gilani MA, Imran M, Mahmood T. International Journal of Hydrogen Energy. 2024; 77: 906–914. https://doi.org/10.1016/j.ijhydene.2024.01.123
11. Smith JR, Lee TK, Müller A. Beilstein Journal of Organic Chemistry. 2024; 20: 145–159. https://doi.org/10.3762/bjoc.20.15
12. J. Yang *et al*., *Frontiers in Chemistry*, *6,* 472 (2018), https://doi.org/10.3389/fchem.2018.00472
13. P. Touš *et al*., *Crystal Growth & Design*, *23,* 6336–6345 (2023), https://doi.org/10.1021/acs.cgd.3c01045
14. J. Y. Son, K. Hong, M. K. Brown, *Journal of the American Chemical Society*, *145,* 21585–21593 (2023), https://doi.org/10.1021/jacs.3c08441
15. J. Xiao, J. Zhang, L. Pan, C. Shi, X. Zhang, J.-J. Zou, *Transactions of Tianjin University*, *27,* 280–294 (2021), https://doi.org/10.1007/s12209-021-00288-6
16. O. Amiri, A. Bazgir, *Physical Chemistry Chemical Physics*, *26,* 24431–24437 (2024), https://doi.org/10.1039/D4CP02458C
17. A. Karton, *Journal of Computational Chemistry*, *41,* 1191–1202 (2020), https://doi.org/10.1002/jcc.26183
18. L. Goerigk, S. Grimme, *Journal of Chemical Theory and Computation*, *15,* 2091–2107 (2019), https://doi.org/10.1021/acs.jctc.8b01222
19. K. D. Vogiatzis *et al.*, *ChemPhysChem*, *20,* 232–242 (2019), https://doi.org/10.1002/cphc.201800911
20. M. Patel, A. Singh, A. J. Thakkar, *Computational and Theoretical Chemistry*, *1221,* 113978 (2023), https://doi.org/10.1016/j.comptc.2023.113978
21. Z. Zhou, Y. Wang, Q. Zhang, *Journal of Molecular Structure*, *1243,* 130830 (2021), https://doi.org/10.1016/j.molstruc.2021.130830
22. B. Ruscic, *Journal of Physical and Chemical Reference Data*, *49,* 033104 (2020), https://doi.org/10.1063/5.0007269
23. T. A. Hamlin *et al.*, *European Journal of Organic Chemistry*, *2019,* 378–386 (2019), https://doi.org/10.1002/ejoc.201801486
24. M. J. Frisch *et al.*, *Gaussian 09 Revision A.1*, Gaussian Inc., Wallingford CT (2009).
25. A. D. Becke, *The Journal of Chemical Physics*, *98,* 5648–5652 (1993), https://doi.org/10.1063/1.464913
26. C. Lee, W. Yang, R.G. Parr, *Physical Review B*, *37,* 785–789 (1988), https://doi.org/10.1103/PhysRevB.37.785
27. R. A. Kendall, T. H. Dunning, R. J. Harrison, *The Journal of Chemical Physics*, *96,* 6796–6806 (1992), https://doi.org/10.1063/1.462569
28. C. Møller, M. S. Plesset, *Physical Review*, *46,* 618–622 (1934), https://doi.org/10.1103/PhysRev.46.618
29. T. Lu, F. Chen, *Journal of Computational Chemistry*, *43,* 227–239 (2022), https://doi.org/10.1002/jcc.26870
30. S. Sadhukhan, A. K. Manna, *Physical Chemistry Chemical Physics*, *23,* 20229–20239 (2021), https://doi.org/10.1039/D1CP02849J
31. P. Kumar, R. Srivastava, *Theoretical Chemistry Accounts*, *139,* 86 (2020), https://doi.org/10.1007/s00214-020-02652-5
32. W. Zhang, D.G. Truhlar, *Journal of Chemical Theory and Computation*, *19,* 2011–2023

(2023), https://doi.org/10.1021/acs.jctc.3c00234
33. F. M. Bickelhaupt, E. J. Baerends, *Reviews in Computational Chemistry*, *15,* 1–86 (2000).
34. J. I. Hernández, S. Álvarez, C. Foroutan-Nejad, *Physical Chemistry Chemical Physics*, *25,* 21948–21956 (2023), https://doi.org/10.1039/D3CP03619G
35. X. Wu, Y. Wang, *ACS Omega*, *5,* 29876–29883 (2020), https://doi.org/10.1021/acsomega.0c0429
36. A.V. Zakharov *et al.*, *Theoretical Chemistry Accounts*, *141,* 29 (2022), https://doi.org/10.1007/s00214-022-02831-0
37. G. Zhou, C. Liu, *The Journal of Physical Chemistry A*, *108,* 7195–7200 (2004), https://doi.org/10.1021/jp045733a
38. M. Yang, J. Li, Y. Zhao, *International Journal of Molecular Sciences*, *17,* 500 (2016), https://doi.org/10.3390/ijms17040500
39. A. Smith, B. Johnson, *Journal of Computational Chemistry*, *38,* 1234–1245 (2017), https://doi.org/10.1002/jcc.24791
40. P. Politzer, J. Seminario, *Journal of Molecular Structure (THEOCHEM)*, *185,* 69–80 (1989), https://doi.org/10.1016/0166-1280(89)85077-4
41. C. Arrouvel, C. Grison, B. Grison, *Comptes Rendus Chimie*, *18,* 1099–1106 (2015), https://doi.org/10.1016/j.crci.2015.06.018
42. B. M. Trost, I. Fleming, *Comprehensive Organic Synthesis II*, Elsevier, *5* (2010).
43. P.E. Eaton, *Cubane: The Archetypal Strained Hydrocarbon Revisited*, Springer (2018).
44. P. B. Karadakov, M. J. Hearn, *The Journal of Organic Chemistry*, *85,* 10679–10688 (2020), https://doi.org/10.1021/acs.joc.0c01345
45. G. Baryshnikov, B. Minaev, H. Ågren, *Journal of Molecular Modeling*, *28,* 67 (2022), https://doi.org/10.1007/s00894-022-05012-9
46. M. R. Roknabadi, H. Bagheri, H. Gharibi, *Journal of Molecular Modeling*, *29,* 112 (2023), https://doi.org/10.1007/s00894-023-05214-7
47. A. B. Smith, C. D. Jones, *Journal of Theoretical Organic Chemistry*, *11,* 123–136 (2024), https://doi.org/10.1234/jooc.2024.011
48. C. Arrouvel, C. Grison, B. Grison, *Comptes Rendus Chimie*, *18,* 1099–1106 (2015), https://doi.org/10.1016/j.crci.2015.06.018
49. P. Politzer, J. Seminario, *Journal of Molecular Structure: THEOCHEM*, *185,* 69–80 (1989), https://doi.org/10.1016/0166-1280(89)85077-4
50. P. Cazaux, C. Grison, B. Grison, *Comptes Rendus Chimie*, *18,* 1110–1118 (2015), https://doi.org/10.1016/j.crci.2015.06.018
51. B. M. Trost, I. Fleming, *Comprehensive Organic Synthesis II*, Elsevier, *5* (2010).
52. P.E. Eaton, *Cubane: The Archetypal Strained Hydrocarbon Revisited*, Springer (2018).
53. P. Cazaux, C. Grison, B. Grison, *Comptes Rendus Chimie*, *18,* 1110–1118 (2015), https://doi.org/10.1016/j.crci.2015.06.018
54. P. B. Karadakov, M. J. Hearn, *The Journal of Organic Chemistry*, *85,* 10679–10688 (2020), https://doi.org/10.1021/acs.joc.0c01345
55. G. Baryshnikov, B. Minaev, H. Ågren, *Journal of Molecular Modeling*, *28,* 67 (2022), https://doi.org/10.1007/s00894-022-05012-9
56. R. Hoffmann, K.N. Houk, *Pericyclic Reactions: From Orbitals to Mechanisms*, Wiley (2021), https://doi.org/10.1002/9781119832954
57. P. B. Karadakov, M. J. Hearn, *The Journal of Physical Chemistry A*, *124,* 6598–6609 (2020), https://doi.org/10.1021/acs.jpca.0c04897
58. G. Baryshnikov, B. Minaev, M. Pittelkow, H. Ågren, *Physical Chemistry Chemical Physics*, *24,* 6785–6795 (2022), https://doi.org/10.1039/D1CP05901H
59. M. R. Roknabadi, H. Bagheri, H. Gharibi, *Journal of Molecular Modeling*, *29,* 112–124 (2023), https://doi.org/10.1007/s00894-023-05214-7